



**Acoustics'08
Paris**
June 29-July 4, 2008

www.acoustics08-paris.org

Metrology and prediction for integrating a subsystem on a vehicle: Application to a fan system attached to the front end of a car

Marie-Hélène Moulet^a, Saul Mapagha^a and Vincent Martin^b

^aCEVAA, Technopole du Madrillet, 2 Rue Joseph Fourier, 76800 Saint Etienne du Rouvray, France

^bInstitut Jean Le Rond d'Alembert, UMR CNRS 7190, UPMC, 2 Place de la Gare de Ceinture, 78210 Saint-Cyr l'Ecole, France
mh.moulet@cevaa.com

The car industry must satisfy physical acoustic and vibratory objectives in order to comply with safety and comfort norms. Among others, efforts entering the chassis should be limited. When a host structure is excited by a vibratory system, called subsystem, it also vibrates and may radiate an acoustic field. Usually, the subsystem is first tested on a bench and the question is then to deduce the efforts entering the chassis from those entering the test bench. Globalising notions of impedance already made evident via elementary deformable structure configurations are used presently through measurements in a technological configuration, the complexity of which does not allow simple modeling. The case of a fan system attached to the front end of a car is under study. Some metrological conclusions, as well as more dedicated ones concerning the fan system itself, will be given. Finally, on the calculation and prediction sides, expected properties that are not satisfied (such as symmetry in measured matrices) are seen to be of no great consequence in the present case.

1 Introduction

The car industry must satisfy physical acoustic and vibratory objectives in order to comply with safety and comfort norms. Among others, efforts entering the chassis should be limited. When a host structure is excited by a vibratory system, called subsystem, it also vibrates and may radiate an acoustic field. Usually, the subsystem is first tested on a bench and the question is then to deduce the efforts entering the chassis from those entering the test bench. Globalising notions of impedance already made evident via elementary deformable structure configurations are used presently through measurements in a technological configuration, the complexity of which does not allow a simple modelling. The case under study is a fan system attached to the front end of a car with two elastic connections on the bottom and two rigid connections on the top. A similar mounting is achieved on an infinitely rigid test bench (a rigid support). The rotating fan is dynamically unbalanced, that induces the force excitation we are interested in. Firstly, forces entering the test bench are measured at the four attach points using a proper instrumentation. The same instrumentation is mounted on the car to measure forces entering the chassis. Because this instrumentation is an intrusive one, measured forces are not rigorously the real forces the fan system applies to the chassis. At the present developmental stage of the study, the main objective is to validate the method using the exact identical instrumentation on both host structures. Then, because the method needs characterisation of the subsystem and of the chassis without the subsystem, a dedicated set-up protocol is introduced. Finally, experimental results are given and prediction forces are compared with measurement results.

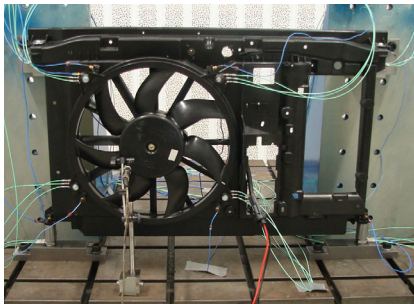


Fig.1. Mounting of the fan system on the test bench.

2 Recall of the strategy

The aim of the study is to deduce the forces applied by a subsystem on a chassis from a measurement of the forces applied by the same subsystem on a test bench (Fig.1). An elastic connection between the host structure (chassis or bench) and the subsystem is present and is modelled by a dynamic stiffness only. The relation between the predicted force vector entering the chassis, denoted \mathbf{f}_c , and the measured force vector entering the test bench, denoted \mathbf{f}_b , is given by [1]:

$$\mathbf{f}_c = \mathbf{Z}'_c(\mathbf{Z}'_m\mathbf{K}'_p\mathbf{Z}'_c + \mathbf{Z}'_c + \mathbf{Z}'_m)^{-1} \times (\mathbf{Z}'_m\mathbf{K}'_p\mathbf{Z}'_b + \mathbf{Z}'_b + \mathbf{Z}'_m)(\mathbf{Z}'_b)^{-1}\mathbf{f}_b \quad (1)$$

where \mathbf{Z}'_m is the dynamic stiffness matrix of the subsystem, \mathbf{Z}'_c is the dynamic stiffness matrix of the chassis, \mathbf{Z}'_b is the dynamic stiffness matrix of the test bench and \mathbf{K}'_p is the dynamic stiffness matrix of the elastic connection. Assuming the test bench is an infinitely rigid test bench, Eq.(1) becomes :

$$\mathbf{f}_c = \mathbf{Z}'_c(\mathbf{Z}'_m\mathbf{K}'_p\mathbf{Z}'_c + \mathbf{Z}'_c + \mathbf{Z}'_m)^{-1}(\mathbf{Z}'_m\mathbf{K}'_p + \mathbf{I})\mathbf{f}_{b\infty} \quad (2)$$

where $\mathbf{f}_{b\infty}$ is the force vector entering the test bench. In practice, measurement of inertances (i.e. the mobility divided by $i\omega$) is usually done. In terms of inertances, Eq.(2) becomes:

$$\mathbf{f}_c = (-\omega^2\mathbf{K}'_p + \mathbf{Y}_m + \mathbf{Y}_c)^{-1}(-\omega^2\mathbf{K}'_p + \mathbf{Y}_m)\mathbf{f}_{b\infty} \quad (3)$$

where \mathbf{Y}_c is the measured inertance matrix of the chassis and \mathbf{Y}_m is the measured inertance matrix of the sub-system. In the following, the predicted force vector \mathbf{f}_c will be compared with a measured force vector \mathbf{f}_{cm} to validate Eq.(3) in the case of an already complex technological object naturally less mastered than an academic configuration. Formulation used in Eq.(1), (2) and (3) is different from the usual canonical form [2] but is obtained by a more straightforward way.

3 Measurement methods

3.1 Measurement of forces

3-Component force sensors are used to measure the twelve components of force vectors at the four attach points between the subsystem and the host structure (car or test bench). The force sensor must be mounted under preload in

order to measure accurately shear forces. Selected mechanical mountings are defined on Fig.2.a for the two attach points at the bottom and Fig.2.b for the two attach points at the top of the fan system. In the studied case, the preload is equal to 15 kN. The top plate, the sensor and the base plate are parts of the host structure. For bottom attach points, a cylindrical piece of the subsystem is inserted into elastic joint, which is put in the host structure. For top attach points, the subsystem is tightened up on the top plate with the same torque the subsystem is tightened up in the car.

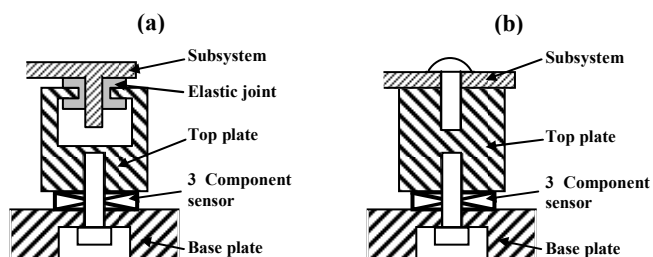


Fig.2. 3D force sensor mounting (case of an elastic connection between the host-structure and subsystem (a), case of a rigid connection between the host-structure and subsystem (b)).

Because the sensor is not at the exact position the subsystem is attached to the host structure, force transfer f_i/f_{Hj} , ($i, j = x, y, z$) between the top of the top plate and the 3-component sensor has to be known (Fig.3.a). Excitation at attach point is done with an impact hammer in the three directions $x, y,$ and z . Then, measured transfer functions are brought together in a matrix whose columns correspond to excitations and lines correspond to responses. In the case of the test bench, respectively the chassis, this matrix is called T_b , respectively T_c . Dimensions of these two matrices are 12×12 . Then the real force vector $f_{b\infty}$ entering the test bench and f_{cm} entering the chassis are deduced from the measured force vectors $f_{b\text{ meas}}$ and $f_{c\text{ meas}}$ by:

$$f_{b\infty} = T_b^{-1} f_{b\text{ meas}} \quad \text{and} \quad f_{cm} = T_c^{-1} f_{c\text{ meas}} \quad (4)$$

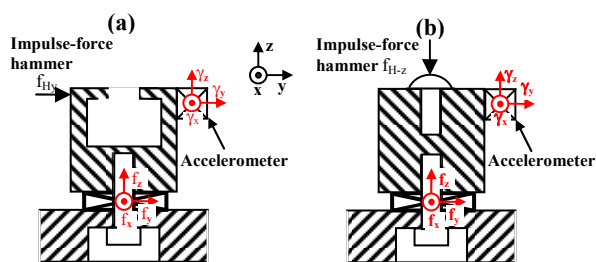


Fig.3. Mounting for force transfer measurement and inertia measurement on the chassis: (a) elastic connection case, (b) rigid connection case.

Fan speed increases from 200 to 3200 rpm. In real use, speed is equal to 3000 rpm. Excitation results from the dynamically unbalanced rotating fan. The first harmonic order is the main one. As a consequence, results will be shown only for this order in the following. Frequency bandwidth is between 10 and 50 Hz (fan speed from 600 to 3000 rpm).

3.2 Measurement of inertances

Needed in Eq.(3), matrices Y_m and Y_c have to be measured. They arise of course from force and acceleration measurements.

Because force sensors and top and base plates are parts of the chassis, 3D accelerometers are glued on one side of the top plate for each attach point to measure terms of Y_c . Excitation is done with an impulse force hammer as close as possible to attach points. The same kind of measurement is done on the test bench to validate that stiffness of the test bench is greater than the stiffness of the fan system, (meaning terms of Y_b are a lot smaller than terms of Y_m) in order to use Eq.(3).

For measurements of terms of Y_m , the fan system is handled using straps to reproduce free conditions (Fig.4). Mountings of accelerometers for top and bottom points are presented on Fig.5.



Fig.4. Mounting of the fan system for Y_m measurement.

For bottom points, the two accelerometers are glued on a surface on which an impact force is applied in x and y directions. For the z direction, the force is applied on the cylindrical piece coming out of the subsystem.

For top points, screws used to fix the subsystem on the chassis are placed in holes and tightened up with the same torque as in the car (10Nm).

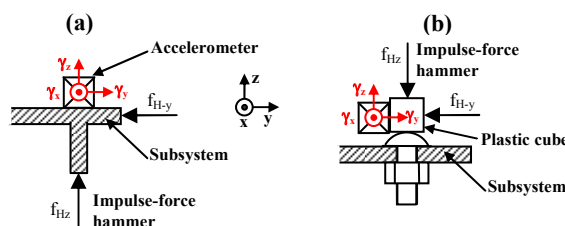


Fig.5. Mounting for inertia measurement on the fan system: (a) bottom points, (b) top points.

4 Measurement results

Names of attach points are shown on Fig.4 and listed below: BL and BR refer to bottom left and bottom right attach points and TL and TR refer to top left and top right attach point. The frame of reference is the one used in a car and shown on Fig.4.

4.1 Forces

Firstly, we present some terms of matrices \mathbf{T}_b and \mathbf{T}_c on Fig.6. As expected, diagonal terms of \mathbf{T}_b are constant and their amplitudes are close to 1. Amplitudes of diagonal terms of \mathbf{T}_c are close to 1 but are not constant except TL z term. Amplitude of terms BL x, TL x and TL y present an increase with frequency caused by a sloshing mode of the top plate on its screw. Amplitude of terms BL y and BL z present a resonance at 33Hz caused by a vibration mode of the front cross member on which force sensors are mounted.

Non-diagonal terms of \mathbf{T}_b are not presented here but are close to 0. On a contrary, some non-diagonal terms of \mathbf{T}_c are different from 0 (especially transfers between y and z directions for the two bottom points) and they have to be considered in the calculation.

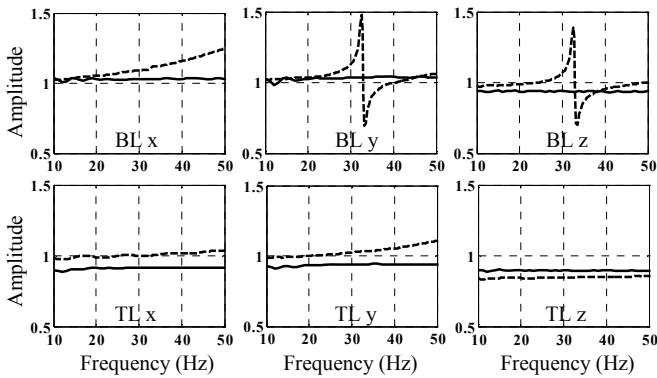


Fig.6. Diagonal terms of matrices \mathbf{T}_b (—) and \mathbf{T}_c (- -).

On Fig 7, components of force vectors $\mathbf{f}_{b\infty}$ and \mathbf{f}_{cm} are compared at points BL and TR. Firstly, for each component of forces, results show amplitudes and phase of $\mathbf{f}_{b\infty}$ and \mathbf{f}_{cm} are of the same magnitude, even if discrepancies exist between these two force vectors: for instance we can see differences of frequencies of the maximum amplitudes of BL y and TR y. In Eq. 3, similar amplitude levels for $\mathbf{f}_{b\infty}$ and \mathbf{f}_{cm} can be explained by the greatness of terms of \mathbf{Y}_m compared with terms of \mathbf{Y}_c and $-\omega^2\mathbf{K}_p^{-1}$ or by the greatness of terms of $-\omega^2\mathbf{K}_p^{-1}$ compared with terms of \mathbf{Y}_c and \mathbf{Y}_m if the model is valid.

Moreover, we can notice components BL z for $\mathbf{f}_{b\infty}$ and \mathbf{f}_{cm} are a lot smaller than other components: there is a 10 dB difference at least. The same result can be seen for components BR z.

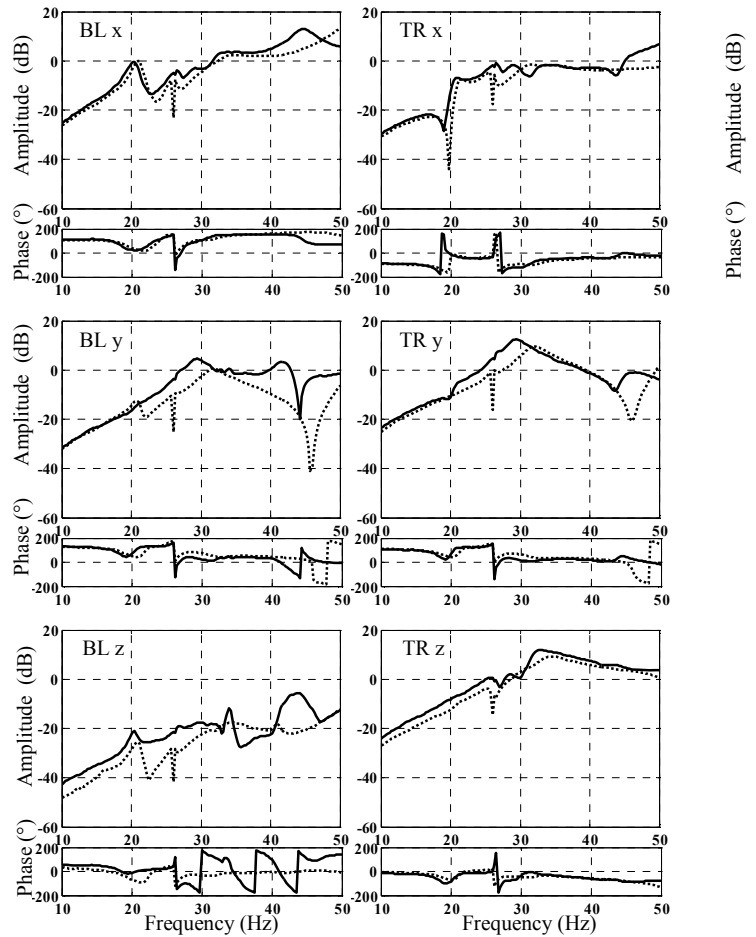


Fig.7: Comparison between measurement of \mathbf{f}_{cm} (—) and measurement of $\mathbf{f}_{b\infty}$ (...).

4.2 Inertances

In this paragraph, γ_i/f_j ($i, j = x, y, z$) ratio is called :

- direct inertance when γ and f are measured at the same point and $i=j$. For instance, measurement in x direction at TL point is written TL x.
- local transfer when γ and f are measured at the same point and $i \neq j$. For instance, local transfer between an acceleration measured in x direction at attach point TL and a force in Y direction at the same point is written TL x/y.
- transfer when γ and f are measured at different points. For instance, a transfer between an acceleration measured in x direction at attach point TR and a force in y direction at point TL is written TR x/ TL y.

Firstly, terms of matrices \mathbf{Y}_m , \mathbf{Y}_c and \mathbf{Y}_b are compared in Fig. 8 for two direct inertances BR x and BL z. These results show terms of \mathbf{Y}_b are much smaller than terms of \mathbf{Y}_m , at least a 45dB difference. The use of Eq.(3) is confirmed. Moreover, we can notice amplitudes of \mathbf{Y}_m terms are greater than amplitudes of \mathbf{Y}_c terms in a large frequency bandwidth. But for some particular frequencies (for example, between 30 and 40 Hz on BL z) terms of \mathbf{Y}_c are greater than terms of \mathbf{Y}_m . As a consequence, we cannot neglect \mathbf{Y}_c matrix in Eq.(3).

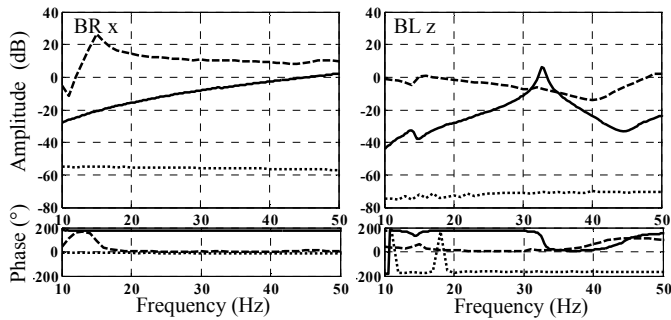


Fig.8: Comparison between direct inertances: subsystem (---), chassis (—) and rigid support (...).

Secondly, reciprocity of measurements has to be validated. Because reciprocity for local transfers is more difficult to obtain than reciprocity for transfers, we represent on Fig. 9 results obtained for local transfers BL z/x and TL y/z for the sub-system. These local transfers are compared with reciprocal measurements BL x/z and TL z/y. This comparison shows property of reciprocity is verified for the subsystem, even if acceleration and force are not measured at the exact same point.

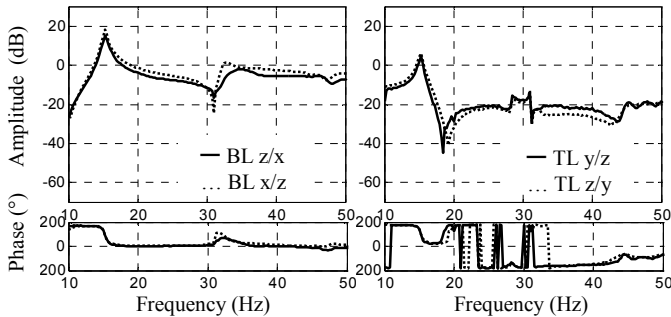


Fig.9: Example of reciprocity of local transfer for Y_m terms.

Fig.10 shows the same kind of results for the chassis. Unlike results for the subsystem, property of reciprocity is not verified for all measurements. As an example, we can see an almost 15dB difference between local transfer BL z/x and BL x/z. The distance between the point where the force is applied and the point where acceleration is measured could explain this discrepancy: the accelerometer may measure an effect due to a rotation movement induced by the excitation. It could explain the fact BL z/x is greater than BL x/z. To avoid this problem, many accelerometers could be glued to separate rotational inertia from the one we are interested in [3].

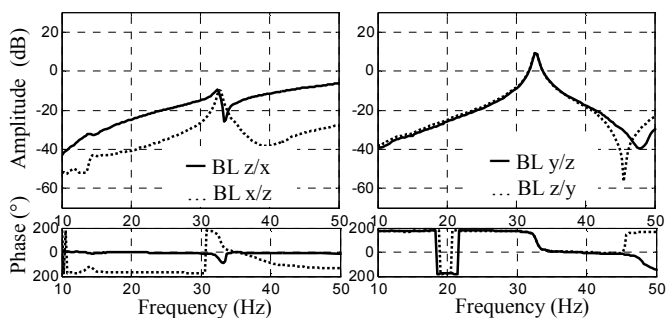


Fig.10: Example of reciprocity of local transfer for Y_c terms.

5 Prediction

In Fig.11, terms of predicted force vector f_c are compared with terms of measured force vectors f_{cm} and $f_{b\infty}$ for BL and TR attach points. The same kind of results is obtained for the two other attach points. Dynamic stiffness matrix K_p , which is used in Eq.3, comes from measurements.

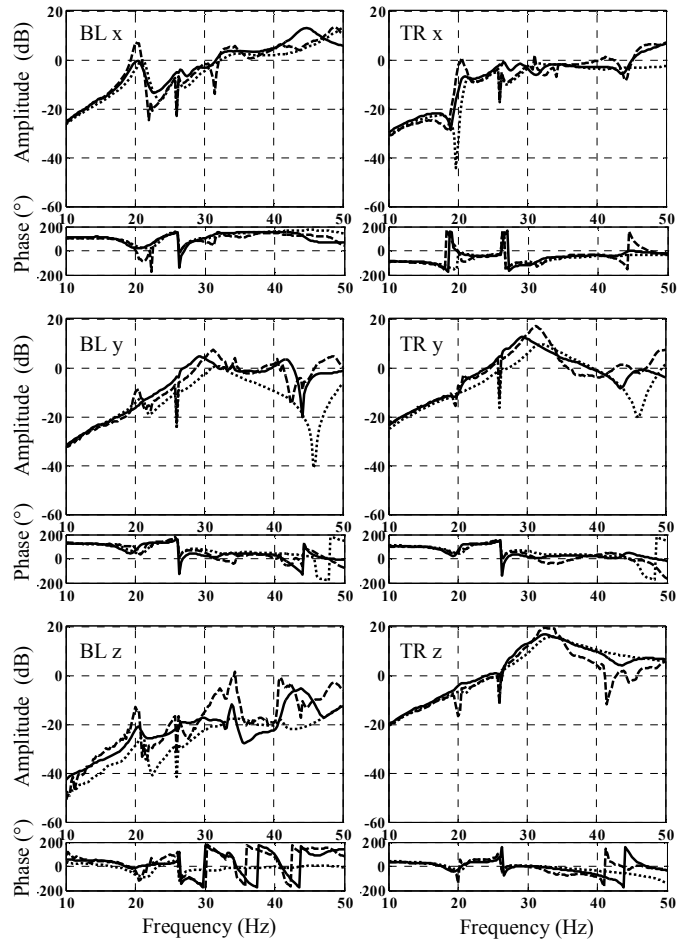


Fig.11: Comparison between prediction of f_c (---), measurement of f_{cm} (—) and measurement of $f_{b\infty}$ (...).

A good agreement exists between predicted values and measured ones. Resonance frequencies of predicted f_c are close to resonance frequencies of measured f_{cm} and frequency gaps, which occurred between components of f_{cm} and components of $f_{b\infty}$, decrease, especially for BL y and TR y.

6 Conclusion

In the technological studied case, we have shown the importance of measuring effort transfer matrices T_b and T_c to obtain accurate values for forces entering the test bench and the chassis. Inertance matrix Y_m is symmetrical, that translates reciprocity of measurements. On the contrary, many arguments could explain why matrix Y_c is not symmetrical: influence of the top plate, the distance between the point where the force is applied and the point where acceleration is measured and rotating motion is not

separated from the translational one. Prediction and measurements show that $\mathbf{f}_{\mathbf{c}_m}$ and $\mathbf{f}_{\mathbf{b}_\infty}$ are almost identical. For the fan system case, we can notice that the rigid support or the chassis are rigid compared with the subsystem and that forces entering the rigid support or the chassis are not very different: as a conclusion, in this case, prediction does not give a lot of information. Nevertheless, this conclusion can be known *a posteriori*.

About metrological conclusions, for the studied case, we showed that if we want to avoid measurement of matrices \mathbf{T}_b and especially \mathbf{T}_c , we should use a high tightening torque and avoid resonance frequencies of the chassis inside the studied frequency range. About inertance measurements, we obtain a good repeatability for all measurements. However, the more the measured term is small, the less repeatability is good: influence of noise measurement is greater in this case.

About \mathbf{f}_c prediction, it should be noticed the small influence on predicted value of the non-symmetry of \mathbf{Y}_c or regularisation methods such as SVD.

If we want to improve the whole method, we should consider rotations in modeling and measurements or not consider them using a dedicated measurement method. In addition, were we able to be really confident in the prediction, the main drawback related to the intrusiveness of the force measurement method on the chassis (which is not the case on the test bench) would no longer deserve attention since there would be no point in the measurement.

References

- [1] V. Martin, S. Mapagha, "Integration of sub-systems on vehicles", *ICSV14*, Cairns, Australia, 9-12 July, 2007
- [2] M. A. Sanderson, "Vibration Isolation: Moments and rotations included", *Journal of Sound and Vibration*, **198**(2), 171-191 (1996)
- [3] D. J. Ewins, "Modal Testing: Theory and Practice", Research Studies Press, 1989